Supplementary Information for

The intrinsic disorder related alloy scattering in ZrNiSn half-Heusler thermoelectric materials

Hanhui Xie[1], Heng Wang[2], Chenguang Fu[1], Yintu Liu[1], G. Jeffrey Snyder[2], Xinbing Zhao[1] and Tiejun Zhu[1,3,*]

[1]*State Key Laboratory of Silicon Materials, Department of Materials Science and Engineering, Zhejiang University, Hangzhou 310027, China, E-mail: zhutj@zju.edu.cn,*

[2] *Department of Materials Science, California Institute of Technology, Pasadena, CA 91125, (USA)*

E-mail: jsnyder@caltech.edu

[3]*Cyrus Tang Center for Sensor Materials and Applications, Zhejiang University, Hangzhou, 310027, China*

To whom correspondence should be addressed: E-mail: zhutj@zju.edu.cn (Tie-Jun Zhu).

1) Sample Information

Table SI The nominal compostions, EPMA compostions and the relative density for $ZrNiSn_{1-x}Sb_x$ samples

Nominal Composition	EPMA Composition	Relative Density
ZrNiSn	$ZrNi_{1.06}Sn_{0.992}$	99.1%
$ZrNiSn_{0.99}Sb_{0.01}$	$ZrNi_{1.05}Sn_{1.03}Sb_{0.015}$	98.1%
$ZrNiSn_{0.98}Sb_{0.02}$	$ZrNi_{1.04}Sn_{1.02}Sb_{0.022}$	99.2%
$ZrNiSn_{0.97}Sb_{0.03}$	$ZrNi_{1.05}Sn_{1.01}Sb_{0.033}$	97.4%
$ZrNiSn_{0.94}Sb_{0.06}$	$ZrNi_{1.06}Sn_{1.00}Sb_{0.063}$	99.2%
$ZrNiSn_{0.92}Sb_{0.08}$	$ZrNi_{1.05}Sn_{0.961}Sb_{0.089}$	98.5%
$ZrNiSn_{0.90}Sb_{0.10}$	$ZrNi_{1.04}Sn_{0.931}Sb_{0.106}$	98.6%

2) XRD patterns of the $ZrNiSn_{1-x}Sb_x$ samples

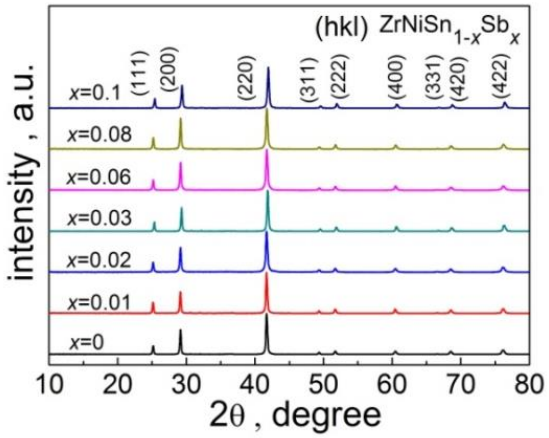

Fig. S1 XRD patterns of the $ZrNiSn_{1-x}Sb_x$ (x = 0 - 0.1) samples. All the XRD patterns can be indexed to the cubic MgAgAs-type half-Heusler crystal structure.

3) The specific heat *C*p

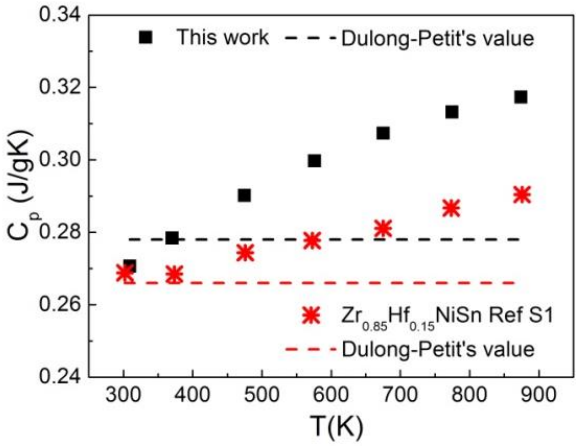

Fig. S2 Temperature-dependent specific heat capacity *C*p for ZrNiSn, compared to

the referenced data [S1].

4) Single Kane Band Model Details

In this paper, acoustic phonon scattering, polar scattering and together with alloy scattering, with the total relaxation time determined by Matthiessen's rule $\tau_{total}^{-1} = \tau_{ac}^{-1} + \tau_{po}^{-1} + \tau_{alloy}^{-1}$, are considered to understand the observed transport properties.

The relaxation time for acoustic phonon scattering based on deformation potential theory [S2] can be expressed as a function of reduced carrier energy $\varepsilon = E/k_B T$:

$$\tau_{ac} = \frac{\pi\hbar^4 v_l^2 \rho N_v}{2^{1/2} m^{*3/2} (k_B T)^{3/2} E_{def}^2} (\varepsilon + \varepsilon^2\alpha)^{-1/2} (1+2\alpha\varepsilon)^{-1} [1 - \frac{8\alpha(\varepsilon+\varepsilon^2\alpha)}{3(1+2\alpha\varepsilon)^2}]^{-1}$$

Here, k_B is the Boltzmann constant, m^* is the total density of state effective mass, N_v is the band degeneracy, v_l is the longitudinal velocity, ρ is the density, E_{def} is the deformation potential which characterizes the change in energy of the electronic band with elastic deformation and thus describes the coupling between phonons and electrons, and $\alpha = k_B T/E_g$, where E_g is the energy gap formed at X point.[S3]

If the lattice contains more than one species of atoms, carriers can also be scattered by the changing polarity due to optical vibration. [S4] At room temperature and above, the polar scattering from optical phonons can be regarded as an elastic process [S5] and therefore a relaxation time can be defined as

$$\tau_{po} = \frac{4\pi\hbar^2 \varepsilon^{1/2} N_v^{1/3}}{2^{1/2} (k_B T)^{1/2} e^2 m_d^{*1/2} (\varepsilon_\infty^{-1} - \varepsilon_0^{-1})} (1+2\alpha\varepsilon)^{-1} (1+\alpha\varepsilon)^{1/2} \{[1 - \delta \ln(1+\frac{1}{\delta})] - \frac{2\alpha\varepsilon(1+\alpha\varepsilon)}{(1+2\alpha\varepsilon)^2}[1 - 2\delta + 2\delta^2 \ln(1+\frac{1}{\delta})]\}^{-1}$$

ε_∞ , ε_0 are the high frequency and static dielectric constants (in F/m), respectively. The measured value $\varepsilon_\infty = 6$ [S6] and calculated $\varepsilon_0 = 26$ [S7] are used here. δ is a function of reduced carrier energy ε defined as:

$$\delta(\varepsilon) = \frac{e^2 m_d^{*1/2} N_v^{2/3}}{2^{1/2} \varepsilon (k_B T)^{1/2} \pi\hbar\varepsilon_\infty} (1+\varepsilon\alpha)^{-1} \times {}^0L_1^{1/2}$$

The generalized Fermi integral ${}^nL_l^m$ is defined by

$${}^nL_l^m = \int_0^\infty (-\frac{\partial f}{\partial \varepsilon}) \varepsilon^n (\varepsilon + \alpha\varepsilon^2)^m (1+2\alpha\varepsilon)^l \, d\varepsilon$$

The relaxation time for alloy disorder was first developed for nondegenerated III-V semiconductors [S8, S9], and the equation for SKB model [S10] can be generalized as:

$$\tau_{\text{alloy}} = \frac{8\hbar^4}{3\sqrt{2}\pi\Omega x(1-x)E_{al}^2 m_b^{*3/2}(k_B T)^{1/2}} \times (\varepsilon+\varepsilon^2\alpha)^{-1/2}(1+2\alpha\varepsilon)^{-1}[1-\frac{8\alpha(\varepsilon+\varepsilon^2\alpha)}{3(1+2\varepsilon\alpha)^2}]^{-1}$$

Here, Here Ω is the volume per atom, x is the concentration ratio of the alloy atom, E_{al} is the alloy scattering potential which determines the magnitude of the alloy scattering for the given alloy, and m_{b}^* is the density-of-state effective mass for a single valley defined as $m^*=N_{\text{v}}^{2/3}m_{\text{b}}^*$.

The transport parameters can be expressed using SKB model. The carrier concentration n:

$$n = \frac{(2m^* k_B T)^{3/2}}{3\pi^2\hbar^3}\int_0^\infty(-\frac{\partial f}{\partial\varepsilon})\varepsilon^{3/2}(1+\varepsilon\alpha)^{3/2}d\varepsilon$$

The drift mobility can be expressed by relaxation time and inertial effective mass defined as $m_I^* = 3(\frac{2}{m_\perp^*}+\frac{1}{m_{\parallel}^*})^{-1}$. In most multi-valley structures, each valley is not spherical in the view of Fermi surfaces. To the first order, these valleys are often approximated as ellipsoids, and effective masses along two principle directions defined as transverse $m_\perp^*$ and longitudinal $m_{\parallel}^*$ components are used.

$$\mu = \frac{e}{m_I^*}\frac{\int_0^\infty(-\frac{\partial f}{\partial\varepsilon})\tau_{total}(\varepsilon+\alpha\varepsilon^2)^{3/2}(1+2\alpha\varepsilon)^{-1}d\varepsilon}{\int_0^\infty(-\frac{\partial f}{\partial\varepsilon})(\varepsilon+\alpha\varepsilon^2)^{3/2}d\varepsilon}$$

The Seebeck coefficient S

$$\alpha = \frac{k_B}{e}(\frac{\int_0^\infty(-\frac{\partial f}{\partial\varepsilon})\tau_{total}\varepsilon^{5/2}(1+\varepsilon\alpha)^{3/2}(1+2\alpha\varepsilon)^{-1}d\varepsilon}{\int_0^\infty(-\frac{\partial f}{\partial\varepsilon})\tau_{total}\varepsilon^{3/2}(1+\varepsilon\alpha)^{3/2}(1+2\alpha\varepsilon)^{-1}d\varepsilon}-\eta)$$

The Hall coefficient A

$$A = \frac{3K(K+2)}{(2K+1)^2}\frac{\int_0^\infty(-\frac{\partial f}{\partial\varepsilon})\tau_{total}\varepsilon^{3/2}(1+\alpha\varepsilon)^{3/2}(1+2\varepsilon\alpha)^{-2}d\varepsilon\int_0^\infty(-\frac{\partial f}{\partial\varepsilon})\tau_{total}\varepsilon^{3/2}(1+\alpha\varepsilon)^{3/2}d\varepsilon}{(\int_0^\infty(-\frac{\partial f}{\partial\varepsilon})\tau_{total}\varepsilon^{3/2}(1+\alpha\varepsilon)^{3/2}(1+2\varepsilon\alpha)^{-1}d\varepsilon)^2}$$

K is the anisotropy factor $K = m^*_{\parallel} / m^*_{\perp}$ of effective mass of the carrier pocket along the two directions. For ZrNiSn system, effective mass associated with the conduction band minimum is found to be highly anisotropic and K=10 was adopted in this work.[S11]

The Lorenz number L is given by

$$L = (\frac{k_B}{e})^2[\frac{\int_0^\infty (-\frac{\partial f}{\partial \varepsilon})\tau_{total}\varepsilon^{7/2}(1+\varepsilon\alpha)^{3/2}(1+2\alpha\varepsilon)^{-1}d\varepsilon}{\int_0^\infty (-\frac{\partial f}{\partial \varepsilon})\tau_{total}\varepsilon^{3/2}(1+\varepsilon\alpha)^{3/2}(1+2\alpha\varepsilon)^{-1}d\varepsilon} - (\frac{\int_0^\infty (-\frac{\partial f}{\partial \varepsilon})\tau_{total}\varepsilon^{5/2}(1+\varepsilon\alpha)^{3/2}(1+2\alpha\varepsilon)^{-1}d\varepsilon}{\int_0^\infty (-\frac{\partial f}{\partial \varepsilon})\tau_{total}\varepsilon^{3/2}(1+\varepsilon\alpha)^{3/2}(1+2\alpha\varepsilon)^{-1}d\varepsilon})^2]$$

as shown in **Fig. S3**. The Lorenz number increase with carrier concentration and gradually moves up towards the degenerated limit.

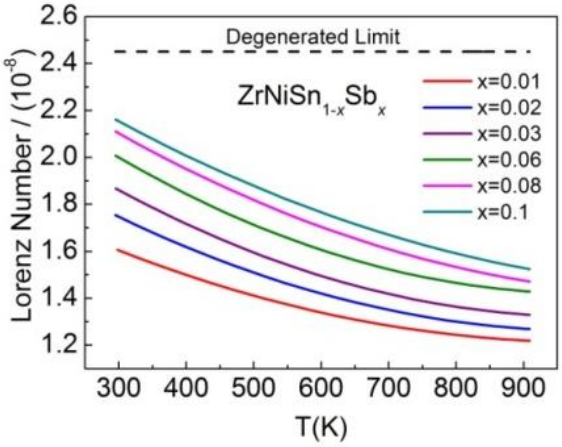

Fig. S3 The temperature dependence of Lorenz number for $ZrNiSn_{1-x}Sb_x$ (x = 0 - 0.1) samples calculated by SKB model

Fig. S4 shows the measured Seebeck coefficient at 300K as a function of Hall carrier density for $ZrNiSn_{1-x}Sb_x$ (x = 0 - 0.1), together with the literature data. [S12-S15] The acoustic phonon scattering and alloy scattering have the same energy dependence with λ=0 and thus gives the same dependence of S vs n_H. The optical scattering causes higher Seebeck coefficient in the low carrier concentration range. At n_H above 10^{20} cm^{-3}, the influence of the optical phonon scattering on S is negligible.

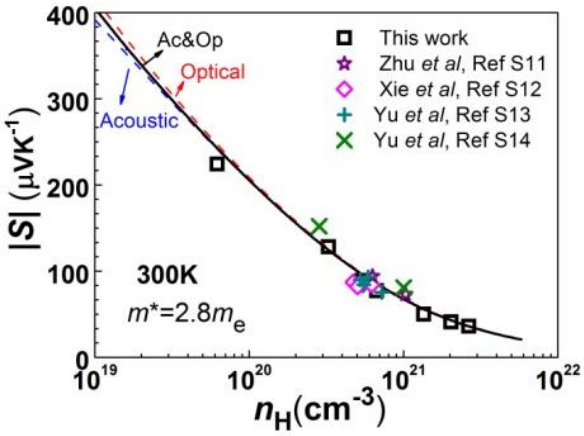

Fig. S4 The Seebeck Coefficient as a function of Hall carrier concentration for $ZrNiSn_{1-x}Sb_x$ (x = 0-0.1) samples. The solid curves are calculated taking into account polar, alloy and acoustic phonon scattering. The dashed lines show the behaviour of each scattering mechanism.

References

S1 S. Chen, K. C. Lukas, W. Liu, C. P. Opeil, G. Chen, Z. Ren, *Adv. Energy Mater.* **2013**, 3, 1210.

S2 C. Herring, E. Vogt, *Phys.Rev.* **1955**, 101, 944.

S3 L. Chaput, J. Tobola, P. Pecheur, H. Scherrer, *Phys. Rev. B* **2006**, 73, 045121.

S4 V. I. Fistul, *Heavily doped Semiconductor*, **1969**, New York, Plenum Press.

S5 Y. I. Ravich, L. Y. Morgovskii, *Sov. Phys. Semiconductors* **1970**, 3, 1278.

S6 F. G. Aliev, A. I. Belogorokhov, N. B. Brandt, V. V. Kozyrkov,R. V. Skolozdra, Y. V. Stadnyk, *JETP Lett.* **1988**, 47, 184.

S7 A. Roy, J. W. Bennett, K. M. Rabe, D. Vanderbilt, *Phys. Rev. Lett.* **2012**, 109, 037602.

S8 J. W. Harrison, J. R. Hauser, *Phys. Rev. B* **1976**, 13, 5347.

S9 J. W. Harrison, J. R. Hauser, *J. Appl. Phys.* **1976**, 47,292.

S10 H. Wang, A. D. LaLonde , Y. Pei and G. J. Snyder, *Adv. Funct. Mater.* **2012**, 23, 1586.

S11 P. Larson and S. D. Mahanti, *Phys. Rev. B* **1999**, 59,15660.

S12 T. J. Zhu, K. Xiao, C. Yu, J. J. Shen, S. H. Yang, A. J. Zhou, X. B. Zhao, J. He, *J. Appl. Phys.* **2010**, 108, 044903.

S13 H. Xie, H. Wang, Y. Pei, C. Fu, X. Liu, G. J. Snyder, X. Zhao and T. Zhu, *Adv. Funct. Mater.* **2013**, 23, 5123.

S14 C. Yu, T. J. Zhu, R. Z. Shi, Y. Zhang, X. B. Zhao, J. He, *Acta Mater.* **2009**, 57, 2757.

S15 C. Yu, H. Xie, C. Fu, T. Zhu, X. Zhao, *J. Mater. Res.* **2012**, 27, 2457.